



## STING Products

The latest buzz in innate immunity

STING Ligands - Variants - Reporter Cells



# Surfactant Protein A Prevents IFN- $\gamma$ /IFN- $\gamma$ Receptor Interaction and Attenuates Classical Activation of Human Alveolar Macrophages

This information is current as of July 26, 2016.

Carlos M. Minutti, Belén García-Fojeda, Alejandra Sáenz, Mateo de las Casas-Engel, Raquel Guillamat-Prats, Alba de Lorenzo, Anna Serrano-Mollar, Ángel L. Corbí and Cristina Casals

*J Immunol* 2016; 197:590-598; Prepublished online 6 June 2016;

doi: 10.4049/jimmunol.1501032

<http://www.jimmunol.org/content/197/2/590>

---

**Supplementary Material** <http://www.jimmunol.org/content/suppl/2016/06/04/jimmunol.1501032.DCSupplemental.html>

**References** This article **cites 53 articles**, 27 of which you can access for free at: <http://www.jimmunol.org/content/197/2/590.full#ref-list-1>

**Subscriptions** Information about subscribing to *The Journal of Immunology* is online at: <http://jimmunol.org/subscriptions>

**Permissions** Submit copyright permission requests at: <http://www.aai.org/ji/copyright.html>

**Email Alerts** Receive free email-alerts when new articles cite this article. Sign up at: <http://jimmunol.org/cgi/alerts/etoc>

---

*The Journal of Immunology* is published twice each month by The American Association of Immunologists, Inc., 9650 Rockville Pike, Bethesda, MD 20814-3994. Copyright © 2016 by The American Association of Immunologists, Inc. All rights reserved. Print ISSN: 0022-1767 Online ISSN: 1550-6606.



# Surfactant Protein A Prevents IFN- $\gamma$ /IFN- $\gamma$ Receptor Interaction and Attenuates Classical Activation of Human Alveolar Macrophages

Carlos M. Minutti,<sup>\*,†,1</sup> Belén García-Fojeda,<sup>\*,†,1</sup> Alejandra Sáenz,<sup>\*,†</sup> Mateo de las Casas-Engel,<sup>‡</sup> Raquel Guillamat-Prats,<sup>†,§</sup> Alba de Lorenzo,<sup>\*</sup> Anna Serrano-Mollar,<sup>†,§</sup> Ángel L. Corbí,<sup>‡</sup> and Cristina Casals<sup>\*,†</sup>

Lung surfactant protein A (SP-A) plays an important function in modulating inflammation in the lung. However, the exact role of SP-A and the mechanism by which SP-A affects IFN- $\gamma$ -induced activation of alveolar macrophages (aM $\phi$ s) remains unknown. To address these questions, we studied the effect of human SP-A on rat and human aM $\phi$ s stimulated with IFN- $\gamma$ , LPS, and combinations thereof and measured the induction of proinflammatory mediators as well as SP-A's ability to bind to IFN- $\gamma$  or IFN- $\gamma$ R1. We found that SP-A inhibited (IFN- $\gamma$  + LPS)-induced TNF- $\alpha$ , iNOS, and CXCL10 production by rat aM $\phi$ s. When rat macrophages were stimulated with LPS and IFN- $\gamma$  separately, SP-A inhibited both LPS-induced signaling and IFN- $\gamma$ -elicited STAT1 phosphorylation. SP-A also decreased TNF- $\alpha$  and CXCL10 secretion by ex vivo-cultured human aM $\phi$ s and M-CSF-derived macrophages stimulated by either LPS or IFN- $\gamma$  or both. Hence, SP-A inhibited upregulation of IFN- $\gamma$ -inducible genes (CXCL10, RARRES3, and ETV7) as well as STAT1 phosphorylation in human M-CSF-derived macrophages. In addition, we found that SP-A bound to human IFN- $\gamma$  ( $K_D = 11 \pm 0.5$  nM) in a Ca<sup>2+</sup>-dependent manner and prevented IFN- $\gamma$  interaction with IFN- $\gamma$ R1 on human aM $\phi$ s. We conclude that SP-A inhibition of (IFN- $\gamma$  + LPS) stimulation is due to SP-A attenuation of both inflammatory agents and that the binding of SP-A to IFN- $\gamma$  abrogates IFN- $\gamma$  effects on human macrophages, suppressing their classical activation and subsequent inflammatory response. *The Journal of Immunology*, 2016, 197: 590–598.

**P**ulmonary surfactant is a lipoprotein complex that lines the alveolar surface. Its main function is to reduce alveolar surface tension (1); however, it also functions as a modulator of immune responses. The two principal surfactant components involved in innate immunity in the alveolus are surfactant protein A (SP-A) and surfactant protein D (2).

SP-A is an oligomeric extracellular protein that is found mainly in the alveolar fluid, associated with surfactant extracellular membranes

that line the alveolar epithelium and with alveolar cells. SP-A recognizes pathogen-associated molecular patterns on some microorganisms, resulting in aggregation, opsonization, or permeabilization of microorganisms and facilitation of microbial clearance (2, 3). Moreover, SP-A is also able to bind to membrane receptors present in macrophages, epithelial cells, and lymphocytes, modifying their response to different stimuli (2). It has been reported that SP-A-deficient mice show decreased microbe clearance from the alveolar space and increased tissue markers of inflammation (4). These findings make SP-A's protective role in alveolar immune defense evident.

The major effector cells of innate immunity in the alveolus are the alveolar macrophages (aM $\phi$ s) that constitute a unique class of professional phagocytes (5). Macrophages change their phenotype reversibly in response to stimuli. This process is called macrophage activation, which varies from classical activation to alternative activation (6, 7). The term "classical activation" refers to macrophages stimulated with IFN- $\gamma$  (host factor) and pathogen products (e.g., TLR agonists such as LPS) (6, 7). IFN- $\gamma$  is the main cytokine associated with classical activation of macrophages. It is mainly produced by Th1 and NK cells and exerts its effects through interactions with its IFN- $\gamma$ R complex, composed of the IFN $\gamma$ R1 and IFN $\gamma$ R2 chains, whose cytoplasmic tails are associated with JAK1 and JAK2 kinases, respectively. IFN- $\gamma$  binds to IFN $\gamma$ R1 with high affinity and activates cross-linking of two molecules of each IFN $\gamma$ R1 and IFN $\gamma$ R2 chain, which results in activation of tyrosine kinases JAK1 and JAK2 and phosphorylation of STAT1. Activated p-STAT1 translocates to the nucleus, where it mediates the transcription of IFN- $\gamma$ -induced genes such as CXCL10 or IFN regulatory factor transcription factors, among others (7, 8). In contrast, the transmembrane TLR4 serves as the primary mediator of LPS signaling, which leads to activation of NF- $\kappa$ B, MAPK, AP-1, IFN

\*Departamento de Bioquímica y Biología Molecular I, Universidad Complutense de Madrid, 28040 Madrid, Spain; <sup>†</sup>Centro de Investigación Biomédica en Red de Enfermedades Respiratorias, Instituto de Salud Carlos III, 28029 Madrid, Spain; <sup>‡</sup>Centro de Investigaciones Biológicas, Consejo Superior de Investigaciones Científicas, 28040 Madrid, Spain; and <sup>§</sup>Departamento de Patología Experimental, Instituto de Investigaciones Biomédicas de Barcelona, Consejo Superior de Investigaciones Científicas, 08036 Barcelona, Spain

<sup>1</sup>C.M.M. and B.G.-F. contributed equally.

ORCID: 0000-0002-9558-3020 (B.G.-F.); 0000-0001-6960-0985 (R.G.-P.); 0000-0002-4990-8162 (A.S.-M.); 0000-0003-2696-0918 (C.C.).

Received for publication May 4, 2015. Accepted for publication May 7, 2016.

This work was supported by Spanish Ministry of Economy and Competitiveness Grants SAF2012-32728 and SAF2015-65307-R (to C.C.) and SAF2014-52423-R (to A.L.C.), Institute of Health Carlos III Grants FIS-PI13/00282 (to A.S.-M.) and CIBERES-CB06/06/0002 (to C.C.), and Fundació Marató de TV3 Grant MTV3 122410 (to A.S.-M.). C.M.M. is a recipient of a fellowship from the Spanish Ministerio de Educación, Cultura y Deporte (Formación de Profesorado Universitario, AP2010-1524).

Address correspondence and reprint requests to Dr. Cristina Casals, Department of Biochemistry and Molecular Biology I, Faculty of Biology, Complutense University of Madrid, 28040 Madrid, Spain. E-mail address: ccasals@ucm.es

The online version of this article contains supplemental material.

Abbreviations used in this article: aM $\phi$ , alveolar macrophage; DLS, dynamic light scattering; ETV7, transcription factor ETV7; HSA, human serum albumin; human M $\phi$ (M-CSF), human monocyte M-CSF-derived macrophage; sIFN- $\gamma$ R1, soluble fraction of IFN- $\gamma$ R1; SP-A, surfactant protein A; RARRES3, retinoic acid receptor responder 3.

Copyright © 2016 by The American Association of Immunologists, Inc. 0022-1767/16/\$30.00

regulatory factors, and early growth response family members, many of which participate in the IFN- $\gamma$  response (9). LPS-stimulated macrophages produce proinflammatory molecules such as TNF- $\alpha$ , IL-1 $\beta$ , and CXCL10, among others (7). IFN- $\gamma$  can “prime” macrophages to give an enhanced response to TLR ligands, such as LPS (10, 11). Synergy between IFN- $\gamma$  and LPS occurs at multiple levels, ranging from signal recognition to convergence of signals at the promoters of target genes (11). Thus, the presence of both IFN- $\gamma$  and TLR ligands induces resting macrophages to rapidly acquire a set of effector functions (production of inflammatory cytokines, chemokines, and reactive oxygen species) that contribute to microbial clearance.

SP-A has been reported to inhibit LPS-induced signaling (p-I $\kappa$ B $\alpha$ , p-ERK, p-p38, and p-Akt) in human monocyte-derived macrophages (12) and to increase expression of the negative regulators of LPS-induced signaling in murine (13) and human monocyte-derived macrophages (14). SP-A also inhibited the production of proinflammatory mediators by human (15) and rat (16, 17) aM $\phi$ s, human monocyte-derived macrophages (18), and human macrophage-like U937 cells (16, 19–21) stimulated with LPS and other TLR ligands. Moreover, SP-A has been reported to modulate aM $\phi$ s responses to IFN- $\gamma$  in the absence or presence of LPS or pathogens, but contradictory observations have also been made. For example, Stämme et al. (22) have shown that SP-A enhances production of NO and iNOS in rat aM $\phi$ s stimulated with IFN- $\gamma$  or IFN- $\gamma$  plus LPS. In contrast, other studies indicate that SP-A suppresses NO production by murine aM $\phi$ s stimulated with IFN- $\gamma$  and IFN- $\gamma$  plus *Mycobacterium avium* (23) or IFN- $\gamma$  plus *Mycobacterium tuberculosis* (24).

To understand the modulatory effects of SP-A on the response of aM $\phi$ s to IFN- $\gamma$  and IFN- $\gamma$  + LPS stimuli [M $\phi$ (LPS/IFN- $\gamma$ )], we studied the effect of SP-A on IFN- $\gamma$ -stimulated human and rat aM $\phi$ s and human M-CSF-derived macrophages [M $\phi$ (M-CSF)] in the absence or presence of LPS. Our data show that SP-A reduces IFN- $\gamma$ -triggered inflammation in rat and human aM $\phi$ s and M $\phi$ (M-CSF). SP-A inhibition of LPS/IFN- $\gamma$ -induced macrophage stimulation is due to SP-A attenuation of both inflammatory agents. To our knowledge, our findings show, for the first time, that SP-A binds to IFN- $\gamma$  preventing IFN- $\gamma$  interaction with IFN- $\gamma$ R1 on the cell surface. We conclude that this could be one of the mechanisms by which SP-A attenuates IFN- $\gamma$  effects.

## Materials and Methods

### Isolation, purification, and characterization of human SP-A

SP-A was isolated from bronchoalveolar lavage of patients with alveolar proteinosis using the sequential butanol and octylglucoside extraction (25, 26). Endotoxin content of isolated human SP-A was  $\sim$ 300 pg endotoxin/mg SP-A as determined by *Limulus* amoebocyte lysate assay (Lonza, Basel, Switzerland). The purity of SP-A was checked by one-dimensional SDS-PAGE in 12% acrylamide under reducing conditions and mass spectrometry. SP-A consisted of supratrimeric oligomers of at least 18 subunits ( $M_r$  650 kDa). The oligomerization state of SP-A was assessed by electrophoresis under nonreducing conditions (25, 26), electron microscopy (26), and analytical ultracentrifugation as reported elsewhere (25). Each subunit had an apparent  $M_r$  36 kDa. Biotinylated SP-A was prepared using the Mini-biotin-XX protein labeling kit (Invitrogen, Carlsbad, CA) as described previously (27). The structure and functional activity of biotinylated SP-A was similar to that of unlabeled SP-A.

### Animal handling and human lung tissue procurement

Rat aM $\phi$ s were obtained from Sprague–Dawley male rat lungs. Rats ( $\sim$ 350 g) were anesthetized with ketamine (80 mg/kg; Merial, Duluth, GA) and xylazine (10 mg/kg; Bayer, Leverkusen, Germany). The cardiopulmonary block was extracted to perform bronchoalveolar lavages with PBS (0.2 mM EDTA). All animals received humane care in accordance with the *Guide for the Care and Use of Laboratory Animals* (28) and Spanish guidelines for experimental animals.

As a source of human lung tissue, we used multiple organ donors. The review board and the ethics committee of the Hospital Clinic of Barcelona, as well as the Spanish and Catalan Transplant Organizations, approved this study, which was conducted in accordance with the guidelines of the World Medical Association's Declaration of Helsinki. Donors with recent history of tobacco smoking, obesity, or any radiological pulmonary infiltrate were excluded from this study. Immediately after obtaining the lungs, we performed a bronchoalveolar lavage at 4°C using 1 l of 0.9% NaCl to isolate human aM $\phi$ s.

### Isolation and culture of primary aM $\phi$ s

Bronchoalveolar cells were separated from lavage fluid by centrifugation ( $250 \times g$ , 7 min). The sedimented cells were washed twice with PBS, and the cell pellet was resuspended in RPMI 1640 medium (10% heat-inactivated

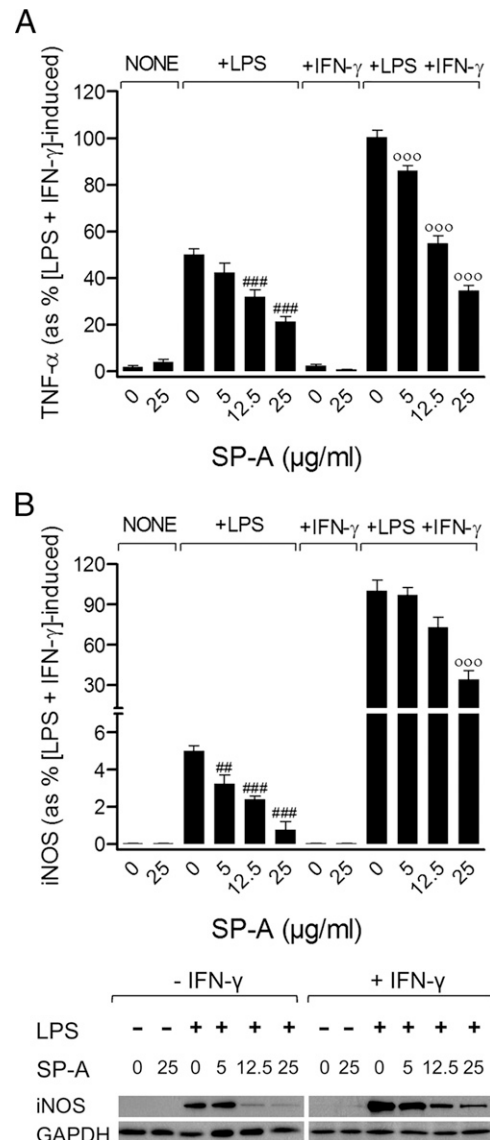


**FIGURE 1.** Inhibitory effect of SP-A on TNF- $\alpha$  and iNOS production by rat alveolar macrophages stimulated with IFN- $\gamma$  and/or LPS. Purified rat aM $\phi$ s were cultured in the presence or absence of IFN- $\gamma$  (10 ng/ml), LPS (1 ng/ml), SP-A (5, 12.5, and 25  $\mu$ g/ml), and combinations thereof. We measured TNF- $\alpha$  secretion by ELISA (**A**) and iNOS production by Western blot (**B**) after 24 h of IFN- $\gamma$  and/or LPS stimulation. The results are expressed as percentage of LPS plus IFN- $\gamma$ -stimulated TNF- $\alpha$  and iNOS production in the absence of SP-A. The mean value of LPS plus IFN- $\gamma$ -induced TNF- $\alpha$  secretion in the absence of SP-A was  $6.8 \pm 0.5$  ng/ml (100%). The data shown are means  $\pm$  SEM of three different aM $\phi$  cultures.  $##p < 0.01$ ,  $###p < 0.001$  when compared with the response elicited by LPS in the absence of SP-A.  $^{\circ\circ\circ}p < 0.001$  when compared with the response elicited by LPS + IFN- $\gamma$  without SP-A.

FBS, 100 U/ml penicillin, and 100  $\mu$ g/ml streptomycin, supplemented with 2 mM glutamine (Lonza). Human and rat aM $\phi$ s were purified by adherence for 90 min at 37°C under a 95% air-5% CO<sub>2</sub> atmosphere in 150-cm<sup>2</sup> culture flasks as reported previously (29, 30). Adherent cells were 94.0  $\pm$  1.1% viable (trypan blue exclusion test). To evaluate the purity of the isolated human macrophages, cells were cytospun in a CytoSpin 3 Cyto centrifuge (Shandon Scientific, Waltham, MA), and the cytospin preparations were stained by Diff-Quick kit (Diagnostics Grifols, Barcelona, Spain) following the manufacturer's protocol. Four fields of each sample were counted. Adherent cells were found to be composed of 94.8  $\pm$  0.8% aM $\phi$ s. In contrast, flow cytometry analysis of rat macrophages immunostained with anti-CD11c (Serotec, Kidlington, U.K.) confirmed the purity of rat aM $\phi$  preparations.

#### Incubation conditions

Adherent cells were gently scraped, plated in 96-well plastic dishes (7.5  $\times$  10<sup>4</sup> cells/well) in 0.2 ml RPMI 1640 medium with 5% FBS, and precultured overnight. Cells were incubated for another 24 h in the presence or absence of smooth LPS (1 ng/ml *Escherichia coli* 055: B5) (Sigma-Aldrich, St. Louis, MO), either rat or human rIFN- $\gamma$  (Calbiochem, Darmstadt, Germany) (0.05–10 ng/ml), human SP-A (5, 12.5, 25, and 50  $\mu$ g/ml), and combinations thereof. Higher doses of both LPS (10–100 ng/ml) and IFN- $\gamma$  (100 ng/ml) were also assayed. At the SP-A concentrations used, the effect of SP-A was greater at lower doses of LPS and/or IFN- $\gamma$  than at higher doses. Cell viability was >97% under assay conditions. Macrophage cultures were plated in triplicate wells, and each series of experiments was repeated at least three times.

#### Generation of M $\phi$ (M-CSF)

Human PBMCs were isolated from buffy coats from normal donors over a lymphoprep gradient (Nycomed Pharma, Oslo, Norway), according to standard procedures. Monocytes were purified from PBMCs by magnetic cell sorting using CD14 microbeads (Miltenyi Biotec, Bergisch Gladbach, Germany). Monocytes (95% CD14<sup>+</sup> cells) were cultured at 0.5  $\times$  10<sup>6</sup> cells/ml for 7 d in RPMI 1640 medium supplemented with 10% FBS at 37°C in a humidified atmosphere with 5% CO<sub>2</sub> and containing M-CSF (ImmunoTools, Friesoythe, Germany) (10 ng/ml) to generate M-CSF-derived macrophages as described previously (31). Cytokines were added every 2 d. Cells were treated with human rIFN- $\gamma$  (1 ng/ml), human SP-A (50  $\mu$ g/ml), and combinations thereof on the eighth day. Cultures were plated in triplicate wells, and each series of experiments was repeated at least three times.

#### Cytokine determinations

Secreted cytokines were quantified in supernatants of treated human and rat aM $\phi$ s using specific ELISA kits following the supplier's instructions. Rat and human TNF- $\alpha$  and human CXCL10 ELISA kits were purchased from BD Biosciences (San Diego, CA) and rat CXCL10 from PeproTech (Rocky Hill, NJ). In brief, Abs were coated on a 96-well Nunc-Immuno Plate MaxiSorp Surface (Thermo Scientific, Waltham, MA) in 0.1 M sodium carbonate (pH 9.5) overnight. After blocking with PBS and 10% FBS and extensive washing, samples and standards were incubated for 2 h at room temperature. Cytokines were detected with biotinylated detection Abs and streptavidin-HRP. The colorimetric reaction was developed with tetramethylbenzidine (BD Biosciences) and was stopped with 4 M sulfuric acid (Sigma-Aldrich), and the absorbance at 450 nm was read on an ELISA reader (DigiScan; Asys HiTech, Eugendorf, Austria).

#### Western blot analysis

Cells were lysed with three freezing-thawing cycles in a buffer containing: 10 mM HEPES (pH 7.9), 15 mM MgCl<sub>2</sub>, 10 mM KCl, 0.5 mM EDTA, 0.2% Triton X-100, 1 mM benzamide, 200  $\mu$ g/ml aprotinin, 200  $\mu$ g/ml leupeptin, and 1 mM PMSF (Sigma-Aldrich). When phosphorylated proteins were analyzed, phosphatase inhibitors were added to the buffer: 20 mM  $\beta$ -glycerophosphate, 10 mM NaF, 10 mM sodium pyrophosphate, and 2 mM orthovanadate (Sigma-Aldrich). Samples were resolved by SDS-PAGE in reducing conditions and transferred to polyvinylidene fluoride membranes (Bio-Rad, Hercules, CA). After blocking with 2.5% skim milk, membranes were washed in PBS and 0.1% Tween and incubated with anti-iNOS, GAPDH, p-ERK, total ERK, p-STAT1, and total STAT1 (Cell Signaling Technology, Danvers, MA). Membranes were incubated with HRP-labeled anti-rabbit IgG (Sigma-Aldrich) and then washed and exposed to ECL reagents (Merk Millipore, Darmstadt, Germany). Immunoreactive bands were densitometered (Quantity One Software; Bio-Rad) and then normalized to GAPDH for iNOS quantification and to the respective total protein for quantification of phosphorylated proteins.

#### Quantitative real-time RT-PCR

Total RNA was extracted using an RNeasy kit from Quiagen (Venlo, The Netherlands), retrotranscribed and amplified in triplicates with the reverse transcription system kit (Applied Biosystems, Waltham, MA) (32). Oligonucleotides for selected genes were designed according to the Universal Probe Library system (Roche Diagnostics, Rotkreuz, Switzerland) for quantitative real-time PCR. The analyses for selected genes were made by Lightcycler 480 (Roche). For quantification of selected genes, the next oligonucleotides were used: 5'-aagcagtttagcaaggaaaggtc-3' and 5'-gacatatactccatgtagggaagtga-3' for *CXCL10*, 5'-gaccacgggggtctgttc-3' and 5'-aaggagcagctgatacacgtaa-3' for *ETV7*, 5'-ctcctcttgcttcgagatg-3' and 5'-aagcggaaaatctcaatca-3' for *RARRES3*, and 5'-agccacatcgctcagacac-3' and 5'-gccaatagcagcaaatcc-3' for *GAPDH*. Levels of mRNA were quantitated using  $\Delta\Delta$ Ct method (33) and were then normalized to maximal expression levels obtained in the presence of IFN- $\gamma$ .

#### Solid-phase binding assays

Solid-phase binding assays were performed as previously described (27) with minor modifications. Either rat IFN- $\gamma$ , human IFN- $\gamma$ , human soluble fraction of IFN- $\gamma$ R1 (sIFN- $\gamma$ R1; R&D Systems, Minneapolis, MN), or human serum albumin (HSA) (Sigma-Aldrich) (1  $\mu$ g/well) was coated on a 96-well Maxisorp microtiter plate in 0.1 mM sodium bicarbonate buffer (pH 9.5)

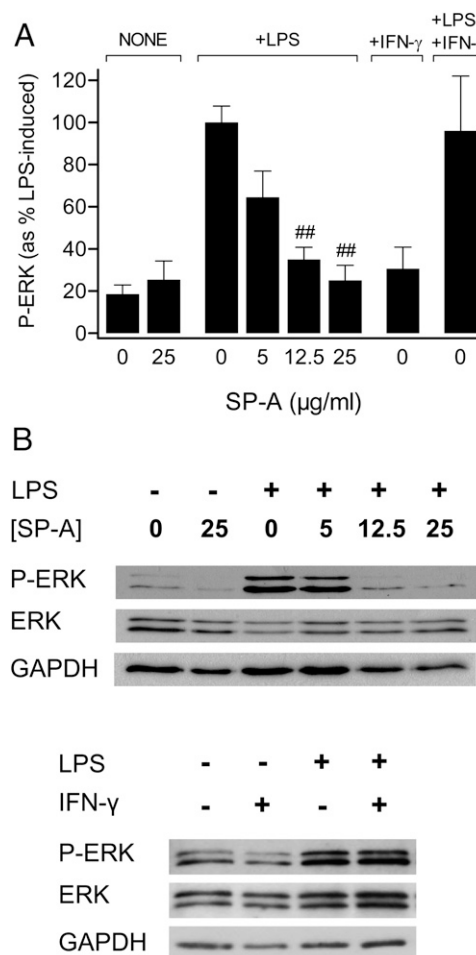


**FIGURE 2.** Inhibitory effect of SP-A on LPS-induced ERK phosphorylation by rat alveolar macrophages. Purified rat aM $\phi$ s were cultured in the presence or absence of LPS (1 ng/ml), IFN- $\gamma$  (10 ng/ml), SP-A (5, 12.5, 25  $\mu$ g/ml), and combinations thereof. We measured ERK phosphorylation by Western blot after 30 min of LPS stimulation in the presence or absence of SP-A or IFN- $\gamma$ . In (A), the results are presented as means ( $\pm$  SEM) from three different aM $\phi$  cultures and expressed as percentages of LPS-induced ERK phosphorylation. <sup>##</sup>*p* < 0.01 when compared with the response elicited by LPS in the absence of SP-A. In (B), representative Western blot images of ERK phosphorylation in rat aM $\phi$ s exposed to either LPS and/or SP-A (upper panel) or LPS and/or IFN- $\gamma$  (lower panel) are shown.

overnight at 4°C. The wells were washed three times with buffer A (5 mM Tris-HCl [pH 7.4] containing 150 mM NaCl) with 0.1 mM EDTA. Wells were blocked with buffer A with 0.1 mM EDTA containing 5% skim milk for 2 h. After the plate was washed, biotinylated SP-A, in concentrations ranging from 0 to 470 nM (0 to 333 µg/ml), was added to the wells in buffer A in the presence or absence of 2 mM CaCl<sub>2</sub>. Incubations were performed for 1 h at room temperature. After extensive washing, streptavidin-HRP (Sigma-Aldrich) was added to the wells. To assay the inhibition of the IFN-γ/sIFN-γR1 interaction by SP-A, the mixture of IFN-γ (0.1 µg/ml) and SP-A (in concentrations ranging from 0 to 160 µg/ml) was added to the sIFN-γR1-coated wells in buffer A, with or without 2 mM CaCl<sub>2</sub>, and incubated at room temperature for 1 h. The binding of IFN-γ to sIFN-γR1 was detected using a polyclonal anti-human IFN-γ (Abcam, Cambridge, U.K.) and HRP-conjugated anti-rabbit Ab. The binding of either biotin-labeled SP-A or anti-human IFN-γ was detected with tetramethylbenzidine. The colorimetric reaction was stopped with 4 M sulfuric acid, and the absorbance was read at 490 nm on an ELISA reader.

### Dynamic light scattering

The hydrodynamic diameters of human and rat IFN-γ, human sIFN-γR1, and human SP-A, as well as mixtures of these components, were determined at 25°C in a Zetasizer Nano S (Malvern Instruments, Malvern, U.K.) equipped with a 633-nm HeNe laser as reported previously (3, 27). Six scans were performed for each sample, and all of the samples were analyzed in triplicate. The interaction of SP-A with IFN-γ in solution was measured by the addition of different SP-A concentrations (from 0 to 150 nM; 0 to 100 µg/ml) to 322 nM (7.7 µg/ml) IFN-γ in buffer A in the absence and presence of 175 µM or 2.5 mM CaCl<sub>2</sub>.

### Binding of [<sup>125</sup>I]-IFN-γ to IFN-γR1 at the cell surface of human aMφs and inhibition by SP-A

Recombinant human IFN-γ was labeled with [<sup>125</sup>I]-Bolton Hunter reagent (PerkinElmer, Waltham, MA) as described previously (34). In brief, 10 µg human IFN-γ in 10 µl 0.1 M sodium borate buffer (pH 8.5) was added to 0.7 mCi [<sup>125</sup>I]-Bolton Hunter reagent, and the reaction mixture was agitated for 15 min at room temperature. The reaction was stopped by the addition of 0.5 ml 0.2 M glycine in 0.1 M borate buffer (pH 8.5) for 5 min at room temperature. Free iodine was separated from the labeled protein using disposable PD-10 desalting columns (GE Healthcare, Waukesha, WI), according to the manufacturer's instructions. The concentration of the

labeled IFN-γ was determined by sandwich-type ELISA by using a polyclonal anti-human IFN-γ, an HRP-conjugated anti-rabbit Ab, and tetramethylbenzidine for color detection.

Human aMφs were plated in 96-well plates (1 × 10<sup>5</sup> cells/well) in 0.2 ml RPMI 1640 medium containing 5% FBS and primed overnight with LPS (1 ng/ml) (37°C, under 5% CO<sub>2</sub> atmosphere). Control wells with no cells were coated with the same medium supplemented with 5% HSA. Subsequently, the cells were washed with PBS. Wells were blocked with PBS plus 0.5% HSA for 30 min at 4°C. After the plate was washed with PBS, [<sup>125</sup>I]-IFN-γ (10 ng/ml) and SP-A (in concentrations ranging from 0 to 100 µg/ml) were added to the cells in RPMI 1640 medium either with 2.5 mM CaCl<sub>2</sub> or with 5 mM EDTA. Incubations were performed for 2 h at 4°C. After extensive washing, the cells were lysed with 10% SDS, and radioactivity was counted with a PerkinElmer Wallac Wizard 1470-020 Gamma Counter. To confirm that the detected [<sup>125</sup>I]-IFN-γ bound specifically to its receptor at the cellular surface, we used a mouse mAb (50 µg/ml) (BD Biosciences), which recognizes the region of human IFN-γR1 that binds to IFN-γ, to inhibit IFN-γ interaction with its receptor (35). An irrelevant, isotype-matched mouse IgG1 mAb (Serotec) was used as a control for these experiments.

### Statistics

Data are presented as means ± SEM. Differences in means between groups were evaluated by one-way ANOVA, followed by the Bonferroni multiple-comparison test. An α level ≤ 5% (*p* ≤ 0.05) was considered significant.

## Results

### SP-A inhibits LPS and IFN-γ effects on rat aMφs

To determine the effects of SP-A on the classical activation of aMφs, primary aMφs isolated from rat lungs were activated with LPS and/or IFN-γ in the absence and presence of SP-A. Fig. 1A and 1B shows that LPS induced significant TNF-α secretion and iNOS expression in rat aMφs and that the induction of both factors was even greater when macrophages were simultaneously incubated with LPS plus IFN-γ. This indicates that IFN-γ treatment results in efficient priming/amplification of TLR4-induced cellular responses. However, IFN-γ alone did not induce TNF-α secretion and iNOS expression in rat aMφs, which is contrary to

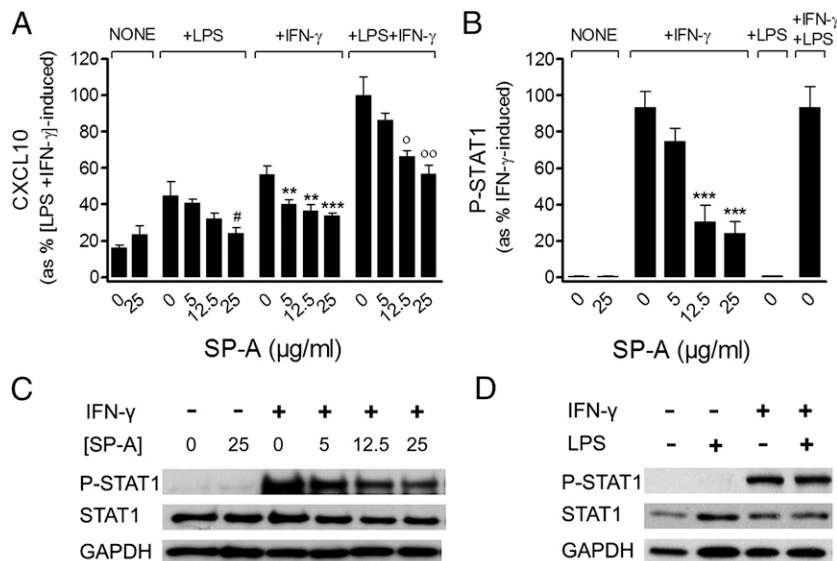


**FIGURE 3.** Inhibitory effect of SP-A on IFN-γ-induced STAT1 Y701 phosphorylation and CXCL10 secretion by rat aMφs. Purified rat aMφs were cultured in the presence or absence of IFN-γ (1–10 ng/ml), LPS (1 ng/ml), SP-A (5, 12.5, 25 µg/ml), and combinations thereof. **(A)** CXCL10 secretion was measured after 24 h IFN-γ (1 ng/ml) and/or LPS stimulation by ELISA. The results are presented as means (± SEM) from three different cell cultures and expressed as percentages of LPS plus IFN-γ-induced CXCL10 secretion. The mean value of LPS plus IFN-γ-induced CXCL10 secretion by rat aMφs in the absence of SP-A was 305 ± 12 pg/ml (100%). **(B)** STAT1 Y701 phosphorylation was measured after 30-min stimulation with IFN-γ (10 ng/ml), LPS (1 ng/ml), or both by Western blot. The data shown are means ± SEM of three different aMφ cultures and were expressed as percentages of IFN-γ-induced STAT1 phosphorylation. **(C and D)** Representative Western blot images of STAT1 phosphorylation in rat aMφs exposed to either IFN-γ (10 ng/ml) and/or SP-A (C) or IFN-γ (10 ng/ml) and/or LPS (1 ng/ml) (D) are shown. #*p* < 0.05 when compared with LPS stimulation without SP-A. \*\**p* < 0.01, \*\*\**p* < 0.001 when compared with the response elicited by IFN-γ alone in the absence of SP-A. °*p* < 0.05, °°*p* < 0.01 when compared with the response elicited by LPS + IFN-γ without SP-A.

previous results in RAW 264.7 peritoneal macrophages cell line (36), where IFN- $\gamma$  upregulates TNF- $\alpha$  and iNOS production.

When different concentrations of SP-A were tested (5, 12.5, and 25  $\mu\text{g/ml}$ ), we found that SP-A significantly inhibited, in a dose-dependent manner, TNF- $\alpha$  secretion (Fig. 1A) and iNOS production (Fig. 1B) by rat aM $\phi$ s stimulated with either LPS alone or LPS plus IFN- $\gamma$ . The effect of SP-A on LPS-stimulated rat aM $\phi$ s is consistent with previous results (15, 16, 19, 20). In line with previous findings (12), SP-A also significantly inhibited LPS-induced phosphorylation of ERK1/2 (T202/Y204) in a dose-dependent manner (Fig. 2), whereas ERK activation was not significantly induced in the presence of either SP-A alone or IFN- $\gamma$  (Fig. 2).

#### SP-A attenuates IFN- $\gamma$ effects on rat aM $\phi$ s

IFN- $\gamma$  signaling is mediated by the cytosolic factor STAT1 that is activated during IFN- $\gamma$ -dependent JAK-STAT activation (11). STAT1 is phosphorylated at two sites (tyrosine 701 and serine 727) following IFN- $\gamma$  exposure (11). To determine whether the inhibitory effect of SP-A on aM $\phi$ s stimulated with LPS plus IFN- $\gamma$  also was due to SP-A attenuation of IFN- $\gamma$ , we measured the effect of SP-A on IFN- $\gamma$ -induced STAT1 Y701 phosphorylation and CXCL10 secretion by rat aM $\phi$ s (Fig. 3).

We found that SP-A dose-dependently inhibited IFN- $\gamma$ -stimulated CXCL10 secretion (Fig. 3A) and STAT1 Y701 phosphorylation (Fig. 3B, 3C) by rat aM $\phi$ s. LPS alone had no effect on STAT1 Y701 phosphorylation after 30 min of LPS stimulation (Fig. 3B, 3D). This was expected because S727, but not Y701, is phosphorylated by p38 MAPK activated by TLR agonists (11). However, LPS alone induced CXCL10 secretion ( $137 \pm 15$  pg/ml) by rat aM $\phi$ s,

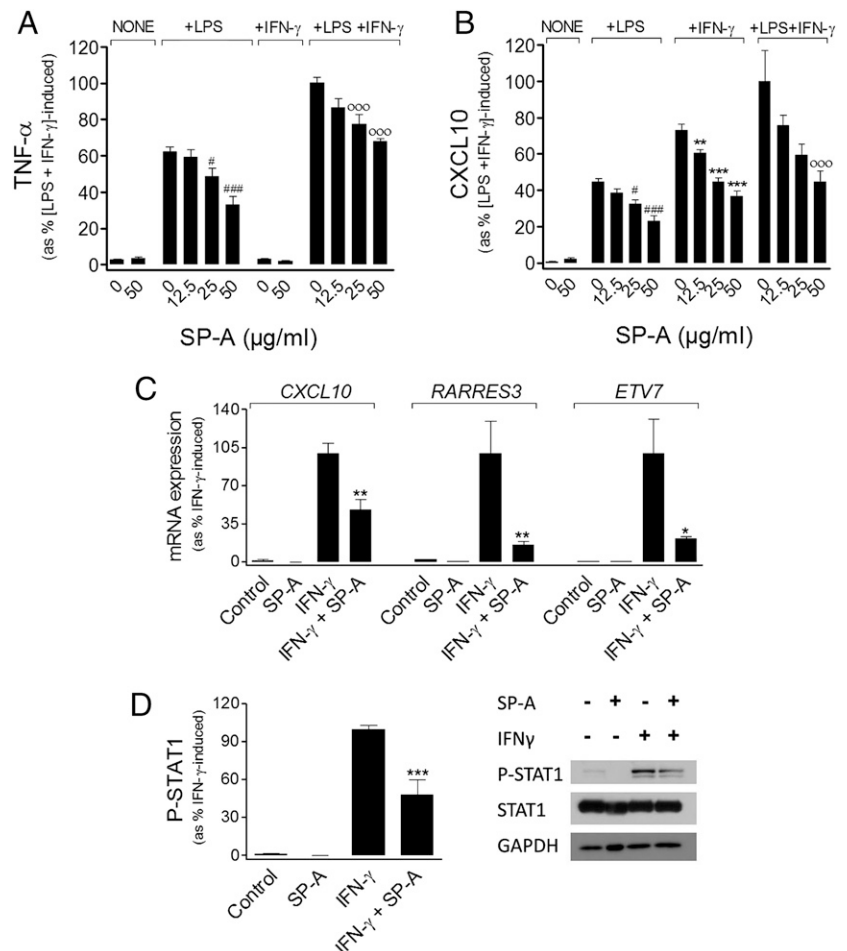
and simultaneous stimulation with LPS plus IFN- $\gamma$  induced higher CXCL10 secretion than with IFN- $\gamma$  alone ( $305 \pm 12$  and  $172 \pm 12$  pg/ml, respectively) (Fig. 3A). The CXCL10 promoter contains response elements for STAT1, NF- $\kappa\text{B}$ , and AP-1 (11), which would explain why aM $\phi$ s produce CXCL10 after stimulation with IFN- $\gamma$  and/or LPS. Secretion of CXCL10 induced by LPS, IFN- $\gamma$ , or LPS plus IFN- $\gamma$  also was inhibited by SP-A in a dose-dependent manner (Fig. 3A), consistent with the results obtained with TNF- $\alpha$  and iNOS described above. Taken together, these data demonstrate that SP-A inhibition of [IFN- $\gamma$  + LPS] stimulation is due to SP-A attenuation of both inflammatory agents.

#### SP-A inhibits LPS and IFN- $\gamma$ effects on ex vivo-cultured human aM $\phi$ s

Given the above set of data on rat aM $\phi$ s, we sought to extend our findings to the case of primary human aM $\phi$ s. Fig. 4A shows that SP-A inhibited TNF- $\alpha$  secretion by human aM $\phi$ s stimulated with LPS alone or LPS plus IFN- $\gamma$  in a dose-dependent manner. Similarly to the observations using rat aM $\phi$ s presented above, IFN- $\gamma$  itself was not capable of significantly stimulating TNF- $\alpha$  secretion. However, IFN- $\gamma$  increased the levels of LPS-induced TNF- $\alpha$  secretion by human aM $\phi$ s, as previously reported (29), and this further increase was significantly impaired by SP-A. Therefore, similar to the case of rat aM $\phi$ s, SP-A is capable of limiting the production of proinflammatory cytokines by human aM $\phi$ s exposed to the classical activation stimuli LPS + IFN- $\gamma$ .

Moreover, as shown in Fig. 4B, SP-A dose dependently inhibited IFN- $\gamma$ -induced CXCL10 secretion by ex vivo cultured human aM $\phi$ s. Simultaneous stimulation with IFN- $\gamma$  and LPS induced higher CXCL10 secretion than with IFN- $\gamma$  alone ( $367 \pm 36$

**FIGURE 4.** Inhibitory effect of SP-A on IFN- $\gamma$  and/or LPS-challenged human macrophages. In (A and B), human aM $\phi$ s were cultured in the presence or absence of IFN- $\gamma$  (1 ng/ml), LPS (1 ng/ml), SP-A (12.5, 25, 50  $\mu\text{g/ml}$ ), and combinations thereof. We measured TNF- $\alpha$  (A) and CXCL10 (B) secretion after 24 h IFN- $\gamma$  and/or LPS stimulation. In (C), human M $\phi$ (M-CSF) were cultured in the presence or absence of IFN- $\gamma$  (1 ng/ml), SP-A (50  $\mu\text{g/ml}$ ), and combinations thereof. We measured CXCL10, RARRES3, and ETV7 induction by real-time quantitative after 24-h IFN- $\gamma$  stimulation. In (D), human M $\phi$ (M-CSF) were cultured in the presence or absence of IFN- $\gamma$  (0.05 ng/ml), SP-A (50  $\mu\text{g/ml}$ ), and combinations thereof. STAT1 Y701 phosphorylation was evaluated by Western blot analysis after 30 min of stimulation. In (A) and (B), the results are expressed as percentage of LPS plus IFN- $\gamma$ -stimulated secretion of TNF- $\alpha$  (A) or CXCL10 (B) in the absence of SP-A. The mean values of LPS plus IFN- $\gamma$ -induced TNF- $\alpha$  and CXCL10 secretion in the absence of SP-A were  $875 \pm 134$  and  $367 \pm 36$  pg/ml, respectively (100%). In (C), results were expressed as percentages of IFN- $\gamma$ -induced gene in the absence of SP-A. In (D), results were expressed as percentages of IFN- $\gamma$ -induced STAT1 phosphorylation. The data shown are means  $\pm$  SEM of three different macrophage cultures.  $^{\#}p < 0.05$ ,  $^{\#\#\#}p < 0.001$  when compared with the response elicited by LPS without SP-A.  $^*p < 0.05$ ,  $^{**}p < 0.01$ ,  $^{***}p < 0.001$  when compared with the response elicited by IFN- $\gamma$  in the absence of SP-A.  $^{ooo}p < 0.001$  when compared with the response elicited by LPS + IFN- $\gamma$  in the absence of SP-A.



and  $268 \pm 16$  pg/ml, respectively), and SP-A also inhibited [LPS + IFN- $\gamma$ ]-induced CXCL10 secretion (Fig. 4B). In contrast, iNOS protein did not increase in response to LPS or LPS plus IFN- $\gamma$  in human aM $\phi$ s (Supplemental Fig. 1). This was expected because little to no iNOS and NO have been detected in human macrophages obtained from normal donors (15, 37), mainly because of epigenetic silencing of NOS2 (38).

#### SP-A inhibits IFN- $\gamma$ effects on human monocyte-derived macrophages M $\phi$ (M-CSF)

We then used human monocyte M-CSF-derived macrophages [human M $\phi$ (M-CSF)]. aM $\phi$ s show phenotypical features of anti-inflammatory macrophages (39) and M-CSF prime monocytes to differentiate into anti-inflammatory macrophages (40). As in the case of ex vivo-cultured human aM $\phi$ s, SP-A inhibited TNF- $\alpha$  and CXCL10 secretion by M $\phi$ (M-CSF) stimulated by LPS, IFN- $\gamma$ , and LPS + IFN- $\gamma$  (Supplemental Fig. 2A, 2B). Human M $\phi$ (M-CSF) stimulated with IFN- $\gamma$  and/or LPS led to higher CXCL10 secretion ( $21.7 \pm 1.5$ ,  $17.4 \pm 2.9$ , and  $13.1 \pm 1.7$  ng/ml in response to LPS + IFN- $\gamma$ , IFN- $\gamma$ , and LPS, respectively) than ex vivo-cultured human aM $\phi$ s ( $367 \pm 36$ ,  $268 \pm 16$ , and  $164 \pm 7$  pg/ml in response to LPS + IFN- $\gamma$ , IFN- $\gamma$ , and LPS, respectively).

CXCL10 is one of the paradigmatic genes induced by IFN- $\gamma$  (11). To find out whether SP-A affected other IFN- $\gamma$ -regulated genes, we evaluated the effect of SP-A on the IFN- $\gamma$ -dependent gene expression in human M $\phi$ (M-CSF). To that end, human M $\phi$ (M-CSF) were stimulated with IFN- $\gamma$  in the presence and absence of SP-A, and IFN- $\gamma$ -induced genes were analyzed by quantitative real-time RT-PCR. Fig. 4C shows that IFN- $\gamma$  upregulated the expression of *CXCL10* (fold change  $65 \pm 6$ ), *RARRES3* (fold change  $34 \pm 13$ ) identified as a retinoic acid responder gene (41), and *ETV7* (fold change  $177 \pm 43$ ) [also known as the human ETS family gene *TEL2/ETV7*, which promotes proliferation and has a role in oncogenesis (42)]. Importantly, SP-A inhibited the IFN- $\gamma$ -induced expression of *CXCL10*, *RARRES3*, and *ETV7* genes by 49, 85, and 70%, respectively (Fig. 4C). Moreover, we found that SP-A inhibited IFN- $\gamma$ -stimulated STAT1 Y701 phosphorylation in human M $\phi$ (M-CSF) (Fig. 4D). Taken together, these findings demonstrate that SP-A also suppressed IFN- $\gamma$  effects in the absence and presence of LPS on human M $\phi$ (M-CSF).

#### SP-A binds to IFN- $\gamma$ and prevents IFN- $\gamma$ binding to its receptor on human aM $\phi$ s

To determine the mechanism by which SP-A diminishes IFN- $\gamma$  effects on rat and human aM $\phi$ s as well as human M $\phi$ (M-CSF), we first studied the potential interaction between SP-A and IFN- $\gamma$  in a solid phase binding assay. Fig. 5A shows that biotinylated SP-A bound to human IFN- $\gamma$ -coated wells in a dose- and Ca<sup>2+</sup>-dependent manner, with  $K_D = 11 \pm 0.5$  nM. Biotinylated SP-A bound neither to IFN- $\gamma$ -coated wells in the absence of Ca<sup>2+</sup> nor to wells coated with human serum albumin nor to wells containing buffer alone, regardless of the presence of Ca<sup>2+</sup>. Biotinylated SP-A also bound to rat IFN- $\gamma$  in a dose- and Ca<sup>2+</sup>-dependent manner with  $K_D = 28 \pm 4$  nM (data not shown). Fig. 5B shows that the percentage of biotinylated SP-A binding to human IFN- $\gamma$ -coated wells decreased by addition of unmodified SP-A, indicating that binding of biotinylated SP-A to IFN- $\gamma$ -coated wells was not because of the biotin moiety.

In addition, the interaction of SP-A with human and rat IFN- $\gamma$  was examined in solution by dynamic light scattering (DLS). Fig. 5C (left panel) shows that human IFN- $\gamma$  alone displays a major peak, which corresponds to particles with a hydrodynamic diameter of  $10.5 \pm 0.5$  nm. The hydrodynamic diameter of human IFN- $\gamma$  determined in these experiments approaches the predicted diameter of  $7 \pm 1$  nm, which does not take into account water

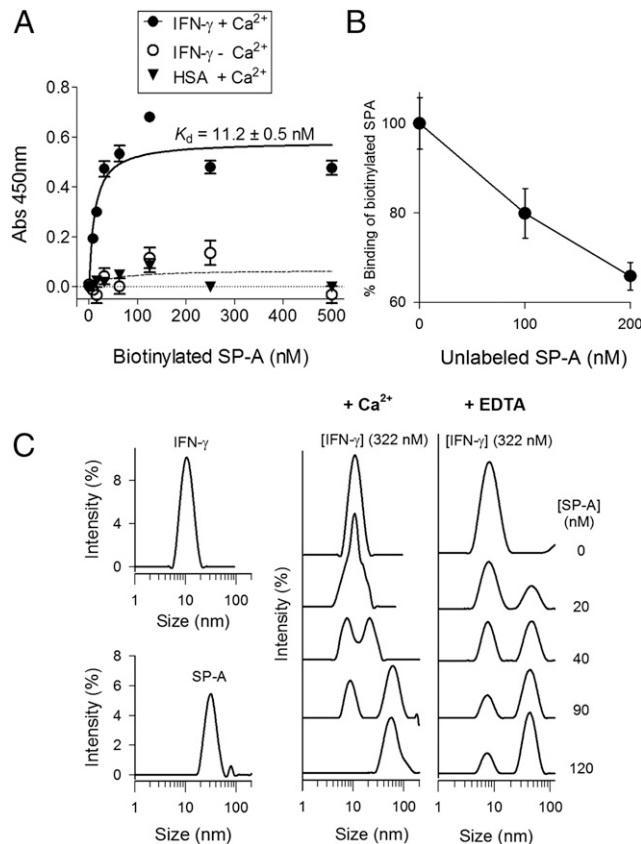


**FIGURE 5.** SP-A binds to IFN- $\gamma$ . (A) Either human IFN- $\gamma$  or HSA (1  $\mu$ g) was coated onto microtiter plate wells. Biotinylated SP-A (0–470 nM; 0–333  $\mu$ g/ml) was then added to the wells in the presence or absence of 2.5 mM Ca<sup>2+</sup>, and levels of bound SP-A were determined with streptavidin-HRP. (B) Competition by unlabeled SP-A of biotinylated SP-A binding to human IFN- $\gamma$ -coated wells. Unlabeled SP-A was added simultaneously with biotinylated SP-A (100 nM; 80  $\mu$ g/ml) to human IFN- $\gamma$ -coated wells (1  $\mu$ g) in presence of 2.5 mM Ca<sup>2+</sup>. In (A) and (B), the data shown are means  $\pm$  SEM of three different experiments. The assays from each SP-A concentration were performed with six independent determinations. (C) DLS analysis of the hydrodynamic diameter of human IFN- $\gamma$  ( $10.5 \pm 0.5$  nm) and SP-A ( $38 \pm 5$  nm). The y-axis represents the relative intensity of the scattered light; the x-axis denotes the hydrodynamic diameter of the particles present in the solution. The analysis of the hydrodynamic diameter of particles after the addition of increasing concentrations of SP-A (0–120 nM; 0–80  $\mu$ g/ml) to a solution containing a constant concentration of IFN- $\gamma$  (322 nM) ( $7.7 \mu$ g/ml) is shown in the presence or absence of calcium. In (C), one representative experiment of three is shown.

molecules enclosing the protein in solution (43). In the case of human SP-A, two identifiable peaks were recognized for SP-A alone, one corresponding to SP-A particles with a hydrodynamic diameter of  $38 \pm 5$  nm and another minor peak corresponding to SP-A aggregates with a hydrodynamic diameter of 1000 nm (data not shown). Self-aggregation of SP-A occurs in a Ca<sup>2+</sup>- and NaCl-dependent manner (44). To reduce SP-A self-aggregation, experiments were performed in the presence of 175  $\mu$ M CaCl<sub>2</sub>.

Fig. 5C (middle panel) shows that the addition of increasing concentrations of SP-A (ranging from 0 to 120 nM; 0 to 80  $\mu$ g/ml) to an IFN- $\gamma$  solution (322 nM) containing calcium caused an SP-A concentration-dependent decrease of the IFN- $\gamma$  peak. At an IFN- $\gamma$ /SP-A molar ratio of  $\sim$ 3:1, only one peak (58 nm) was observed with a hydrodynamic diameter higher than those of SP-A and IFN- $\gamma$  alone. This new peak likely consists of SP-A/IFN- $\gamma$  complexes. This peak did not appear in the absence of Ca<sup>2+</sup> (Fig. 5C, right panel). Similar results were obtained with rat IFN- $\gamma$  (data not

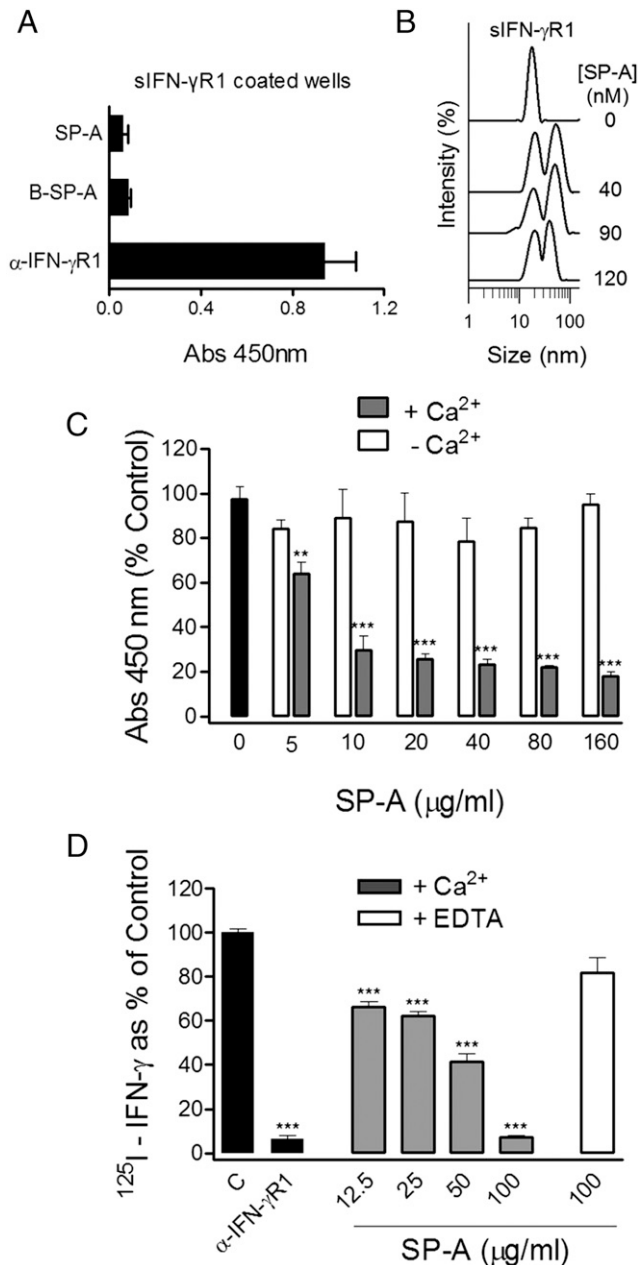


**FIGURE 6.** SP-A prevents IFN- $\gamma$  interaction with IFN- $\gamma$ R1 (IFN- $\gamma$ R1/CD119). **(A)** sIFN- $\gamma$ R1 (1  $\mu$ g) was coated onto microtiter wells. Coated sIFN- $\gamma$ R1 was detected using rabbit polyclonal anti-human IFN- $\gamma$ R1. Either biotinylated (B-SP-A) or unlabeled SP-A (160  $\mu$ g/ml) was incubated for 1 h in the presence of 2.5 mM Ca<sup>2+</sup>. SP-A binding to coated sIFN- $\gamma$ R1 was determined with streptavidin-HRP. **(B)** DLS analysis of the hydrodynamic diameter of particles after the addition of increasing concentrations of SP-A (0–80  $\mu$ g/ml) to a solution containing a constant concentration of sIFN- $\gamma$ R1 (5  $\mu$ g/ml). **(C)** sIFN- $\gamma$ R1 (1  $\mu$ g) was coated onto microtiter wells. IFN- $\gamma$  (100 ng/ml) and different concentrations of SP-A (0–160  $\mu$ g/ml) in the presence or absence of 2.5 mM Ca<sup>2+</sup> were incubated for 1 h. The binding of IFN- $\gamma$  to sIFN- $\gamma$ R1-coated wells was detected using a polyclonal anti-human IFN- $\gamma$  and HRP-conjugated anti-rabbit Ab. \*\* $p$  < 0.01, \*\*\* $p$  < 0.001, when compared with IFN- $\gamma$  binding without SP-A (defined as 100%). **(D)** LPS-primed human aM $\phi$ s were blocked and incubated with [<sup>125</sup>I]-IFN- $\gamma$  (10 ng/ml) and SP-A (at concentrations ranging from 0 to 100  $\mu$ g/ml) with either 2.5 mM CaCl<sub>2</sub> or 2.5 mM EDTA. Incubations were performed for 2 h at 4°C. Cells were lysed with 10% SDS, and radioactivity was measured. Human aM $\phi$ s incubated with anti-IFN- $\gamma$ R1 Ab were used as a positive control to prevent interaction between IFN- $\gamma$  and its receptor. The gamma counts of IFN- $\gamma$  binding without SP-A were defined as 100%. The data are means  $\pm$  SEM

shown). Therefore, this set of experiments demonstrates that SP-A and IFN- $\gamma$  interact in solution in a Ca<sup>2+</sup>-dependent manner.

To clarify whether SP-A has a direct effect on IFN- $\gamma$ -induced cell response by interacting not only with IFN- $\gamma$  but also with its cellular receptor, the extracellular domain of IFN- $\gamma$ R1 (sIFN- $\gamma$ R1) was coated onto microtiter plate wells. Biotinylated SP-A was then added to the wells, and the level of bound SP-A was determined with streptavidin-HRP. No detectable binding of SP-A to sIFN- $\gamma$ R1 was observed (Fig. 6A). In addition, no detectable SP-A/sIFN- $\gamma$ R1 interaction was observed in solution when examined by DLS (Fig. 6B).

To determine whether SP-A interferes with the binding of IFN- $\gamma$  to its receptor, IFN- $\gamma$  binding to coated sIFN- $\gamma$ R1 was determined by ELISA using a polyclonal anti-human IFN- $\gamma$  and in the presence and absence of SP-A (Fig. 6C). We found that SP-A interfered with the binding of IFN- $\gamma$  to IFN- $\gamma$ R1 in the presence but not the absence of Ca<sup>2+</sup>. The inhibition caused by SP-A was saturable and dose and Ca<sup>2+</sup> dependent, with a ~80% inhibition at concentrations  $\geq$  20  $\mu$ g/ml (30 nM). As expected, the binding of IFN- $\gamma$  to its receptor IFN- $\gamma$ R1 was not affected by Ca<sup>2+</sup> (data not shown).

We next examined whether SP-A could effectively inhibit the binding of IFN- $\gamma$  to IFN- $\gamma$ R1 on the cell surface. To achieve this, we analyzed the binding of [<sup>125</sup>I]-IFN- $\gamma$  to IFN- $\gamma$ R1 on human aM $\phi$ s. To confirm that the detected [<sup>125</sup>I]-IFN- $\gamma$  bound specifically to its receptor at the cellular surface, we used a mAb (mouse anti-human CD119) that recognizes the region of IFN- $\gamma$ R1 that binds to IFN- $\gamma$  to block [<sup>125</sup>I]-IFN- $\gamma$  binding to its receptor. Fig. 6D shows that, in the absence of SP-A, [<sup>125</sup>I]-IFN- $\gamma$  bound to human aM $\phi$ s and that this binding was specifically abrogated by the blocking Ab. Conversely, an isotype-matched mouse IgG1 control did not inhibit [<sup>125</sup>I]-IFN- $\gamma$  binding to human aM $\phi$ s (data not shown). However, addition of SP-A clearly inhibited the [<sup>125</sup>I]-IFN- $\gamma$  binding to IFN- $\gamma$ R1 in a dose-dependent manner in the presence but not absence of calcium. Similar results were found on rat aM $\phi$ s. Therefore, our results indicate that SP-A impairs IFN- $\gamma$  recognition by IFN- $\gamma$ R1 on the cell surface. This could be at least one of the mechanisms by which SP-A suppresses IFN- $\gamma$  effects.

## Discussion

Innate immune defense in the alveolar space is characterized by a delicate balance between an effective inflammatory response and the maintenance of tissue integrity. aM $\phi$ s play a major role in this equilibrium by producing and releasing a variety of biologically active products in response to stimuli such as LPS and IFN- $\gamma$  (5, 39). Macrophage activation and the initiation of inflammation involve a complex balancing act between activating and repressing signals. The results of the current study show that SP-A has an anti-inflammatory effect on rat and human aM $\phi$ s and human M $\phi$ (M-CSF), counteracting the stimulation exerted by IFN- $\gamma$  or LPS + IFN- $\gamma$ .

In this study, we have shown that SP-A, used at concentrations within the ranges found in healthy individuals (15–105  $\mu$ g/ml) (45), inhibited the production of proinflammatory molecules such as TNF- $\alpha$  and CXCL10 by rat and human aM $\phi$ s and human M $\phi$ (M-CSF) stimulated with IFN- $\gamma$ , LPS, and LPS + IFN- $\gamma$ . SP-A also inhibited iNOS production by rat aM $\phi$ s stimulated with LPS and LPS + IFN- $\gamma$ . iNOS production by stimulated human aM $\phi$ s was not detected,

of three different experiments [with different human aM $\phi$  cultures in (D)]. The assays from each macrophage preparation were performed with triplicate determinations. \*\* $p$  < 0.01, \*\*\* $p$  < 0.001, when compared with IFN- $\gamma$  binding to its receptor in the absence of SP-A.



confirming previous results that indicate that human aMφs and blood-monocyte-derived macrophages obtained from normal donors and stimulated *in vitro* generally do not express iNOS (15, 37, 38). SP-A also inhibited IFN- $\gamma$ -induced STAT1 phosphorylation in rat aMφs and human Mφ(M-CSF) and inhibited upregulation of IFN- $\gamma$ -inducible genes (*CLCX10*, *RARRES3*, and *ETV7*) by human Mφ(M-CSF). In addition, to our knowledge, we have shown for the first time that human SP-A bound to IFN- $\gamma$  with high affinity ( $K_D = 11 \pm 0.5$  nM for human IFN- $\gamma$  and  $K_D = 28 \pm 4$  nM for rat IFN- $\gamma$ ) and prevented IFN- $\gamma$  interaction with its receptor IFN- $\gamma$ R1 on human aMφs. These data disclose a novel mechanism by which SP-A controls inflammation in the alveolus.

Our observation that SP-A reduces IFN- $\gamma$ -triggered inflammation in rat and human aMφs and human Mφ(M-CSF) is in agreement with the previous studies that showed that SP-A suppresses NO production by murine aMφs stimulated with IFN- $\gamma$  and IFN- $\gamma$  plus *M. avium* (23) or IFN- $\gamma$  plus *M. tuberculosis* (24). However, our results appear to contradict the data from Stämme et al. (22) using rat aMφs. We do not currently have a clear explanation for these contrasting results, although there might be some differences in the experimental design. For instance, starting cell number, media and supplements, different types of plastic, and other conditions such as whether macrophages are rested prior to activation might have substantial effects on activation status. In addition, the source and concentration of cytokines is also important.

aMφs reside in a tissue compartment that is constantly exposed to contaminated air. Thus, aMφ activation is tightly controlled through several cell–cell and soluble mediator interactions to limit unwanted inflammatory responses (39). SP-A is one of the soluble factors that contribute to create an anti-inflammatory state in the lungs through various mechanisms. First, SP-A blocks the binding of TLR ligands to their receptors by direct SP-A interaction with TLR4 (21), TLR2 (16), the TLR coreceptor MD2 (21), and CD14 (19, 20). Second, SP-A modifies macrophage response to TLR ligands by modulating signaling cascades. For example, SP-A increases the expression of negative regulators of TLR signaling, such as IRAK-M (14) and  $\beta$ -arrestin 2 (13), thereby inhibiting LPS-induced stimulation of macrophages. Moreover, SP-A promotes protein kinase C $\zeta$  activation and I $\kappa$ B $\alpha$  stabilization through mechanisms that require SP-A endocytosis by macrophages (17). Internalized SP-A also inhibits I $\kappa$ B $\alpha$ , ERK, p38, and Akt phosphorylation by macrophages stimulated with TLR2 and TLR4 ligands (12). Third, SP-A reduces the production of reactive oxygen intermediates by inhibiting NADPH oxidase activity in human monocyte-derived macrophages activated by PMA or serum-opsonized zymosan (18). In this study, we showed that the binding of SP-A to IFN- $\gamma$ , which suppressed IFN- $\gamma$  interaction with its receptor IFN- $\gamma$ R at the cell surface, is another mechanism by which SP-A limits inflammation and maintains a tolerant lung environment in the steady state. However, following an infection, a harsh IFN- $\gamma$  induction would potentially override SP-A capability to block IFN- $\gamma$ , leading to a desirable inflammatory response to fight against infection. The fact that SP-A is induced in response to IFN- $\gamma$  (46) suggests that SP-A may also be implicated in the regulation of detrimental inflammation at the resolution phase postinfection.

IFN- $\gamma$  is essential for antimycobacterial immunity, and disorders of IFN- $\gamma$  production confer predisposition to mycobacterial disease in humans (47). However, high levels of secreted IFN- $\gamma$  may be harmful. It has been shown that IFN- $\gamma$  and IFN- $\gamma$ -induced CXCL10 are directly involved in the exacerbation of different lung inflammatory diseases (acute lung injury and bronchiolitis)

in murine experimental models and/or humans (48, 49). Moreover, IFN- $\gamma$  causes emphysema and alterations in pulmonary protease/antiprotease balance when expressed in pulmonary tissues (50). Furthermore, the administration of neutralizing Abs against IFN- $\gamma$  or CXCL10 has been shown to attenuate lung injury and/or improve mice survival rate (51, 52).

The alveolar fluid from normal lungs contains high concentrations of SP-A that probably minimize the biological effects of low concentrations of endotoxins that enter the alveolus and IFN- $\gamma$ . In patients with acute lung injury in which proinflammatory cytokines and neutrophils accumulate in the air spaces, the concentration of SP-A significantly decreases (53, 54). The observation that SP-A restores lung tissue integrity in response to sterile inflammation (55) supports the hypothesis that SP-A may be important in modulating inflammation and epithelial integrity in the lung in response to acute injury.

In summary, we have shown that human SP-A inhibits IFN- $\gamma$ , LPS, and LPS + IFN- $\gamma$  effects on rat and human aMφs and human Mφ(M-CSF) and that SP-A binds to IFN- $\gamma$  with high affinity, inhibiting IFN- $\gamma$  recognition by its receptor on the cell surface. These data unravel a previously unknown mechanism by which SP-A/IFN- $\gamma$  interaction plays a significant role in tipping the balance of inflammation to protect the alveolar epithelium.

## Acknowledgments

We thank the main facility of the Faculty of Biology and the Radioactivity Unit of the Faculty of Medicine of Universidad Complutense de Madrid for excellent technical support. In addition, we thank Dr. Begoña García-Álvarez for advice.

## Disclosures

The authors have no financial conflicts of interest.

## References

- Casals, C., and O. Cañadas. 2012. Role of lipid ordered/disordered phase coexistence in pulmonary surfactant function. *Biochim. Biophys. Acta* 1818: 2550–2562.
- Wright, J. R. 2005. Immunoregulatory functions of surfactant proteins. *Nat. Rev. Immunol.* 5: 58–68.
- Coya, J. M., H. T. Akinbi, A. Sáenz, L. Yang, T. E. Weaver, and C. Casals. 2015. Natural anti-infective pulmonary proteins: *in vivo* cooperative action of surfactant protein SP-A and the lung antimicrobial peptide SP-BN. *J. Immunol.* 195: 1628–1636.
- LeVine, A. M., and J. A. Whitsett. 2001. Pulmonary collectins and innate host defense of the lung. *Microbes Infect.* 3: 161–166.
- Kopf, M., C. Schneider, and S. P. Nobs. 2015. The development and function of lung-resident macrophages and dendritic cells. *Nat. Immunol.* 16: 36–44.
- Martinez, F. O., and S. Gordon. 2014. The M1 and M2 paradigm of macrophage activation: time for reassessment. *F1000Prime Rep.* 6: 13.
- Murray, P. J., J. E. Allen, S. K. Biswas, E. A. Fisher, D. W. Gilroy, S. Goerdt, S. Gordon, J. A. Hamilton, L. B. Ivashkiv, T. Lawrence, et al. 2014. Macrophage activation and polarization: nomenclature and experimental guidelines. *Immunity* 41: 14–20.
- Schroder, K., P. J. Hertzog, T. Ravasi, and D. A. Hume. 2004. Interferon- $\gamma$ : an overview of signals, mechanisms and functions. *J. Leukoc. Biol.* 75: 163–189.
- Brubaker, S. W., K. S. Bonham, I. Zanoni, and J. C. Kagan. 2015. Innate immune pattern recognition: a cell biological perspective. *Annu. Rev. Immunol.* 33: 257–290.
- Hu, X., J. Chen, L. Wang, and L. B. Ivashkiv. 2007. Crosstalk among Jak-STAT, Toll-like receptor, and ITAM-dependent pathways in macrophage activation. *J. Leukoc. Biol.* 82: 237–243.
- Schroder, K., M. J. Sweet, and D. A. Hume. 2006. Signal integration between IFN $\gamma$  and TLR signalling pathways in macrophages. *Immunobiology* 211: 511–524.
- Henning, L. N., A. K. Azad, K. V. Parsa, J. E. Crowther, S. Tridandapani, and L. S. Schlesinger. 2008. Pulmonary surfactant protein A regulates TLR expression and activity in human macrophages. *J. Immunol.* 180: 7847–7858.
- Sender, V., L. Lang, and C. Stämme. 2013. Surfactant protein-A modulates LPS-induced TLR4 localization and signaling via  $\beta$ -arrestin 2. *PLoS One* 8: e59896.
- Nguyen, H. A., M. V. Rajaram, D. A. Meyer, and L. S. Schlesinger. 2012. Pulmonary surfactant protein A and surfactant lipids upregulate IRAK-M, a negative regulator of TLR-mediated inflammation in human macrophages. *Am. J. Physiol. Lung Cell. Mol. Physiol.* 303: L608–L616.

15. Arias-Diaz, J., I. Garcia-Verdugo, C. Casals, N. Sanchez-Rico, E. Vara, and J. L. Balibrea. 2000. Effect of surfactant protein A (SP-A) on the production of cytokines by human pulmonary macrophages. *Shock* 14: 300–306.
16. Murakami, S., D. Iwaki, H. Mitsuizawa, H. Sano, H. Takahashi, D. R. Voelker, T. Akino, and Y. Kuroki. 2002. Surfactant protein A inhibits peptidoglycan-induced tumor necrosis factor- $\alpha$  secretion in U937 cells and alveolar macrophages by direct interaction with Toll-like receptor 2. *J. Biol. Chem.* 277: 6830–6837.
17. Moulakakis, C., and C. Stamme. 2009. Role of clathrin-mediated endocytosis of surfactant protein A by alveolar macrophages in intracellular signaling. *Am. J. Physiol. Lung Cell. Mol. Physiol.* 296: L430–L441.
18. Crowther, J. E., V. K. Kutala, P. Kuppusamy, J. S. Ferguson, A. A. Beharka, J. L. Zweier, F. X. McCormack, and L. S. Schlesinger. 2004. Pulmonary surfactant protein A inhibits macrophage reactive oxygen intermediate production in response to stimuli by reducing NADPH oxidase activity. *J. Immunol.* 172: 6866–6874.
19. Sano, H., H. Sohma, T. Muta, S. Nomura, D. R. Voelker, and Y. Kuroki. 1999. Pulmonary surfactant protein A modulates the cellular response to smooth and rough lipopolysaccharides by interaction with CD14. *J. Immunol.* 163: 387–395.
20. Garcia-Verdugo, I., F. Sánchez-Barbero, K. Soldau, P. S. Tobias, and C. Casals. 2005. Interaction of SP-A (surfactant protein A) with bacterial rough lipopolysaccharide (Re-LPS), and effects of SP-A on the binding of Re-LPS to CD14 and LPS-binding protein. *Biochem. J.* 391: 115–124.
21. Yamada, C., H. Sano, T. Shimizu, H. Mitsuizawa, C. Nishitani, T. Himi, and Y. Kuroki. 2006. Surfactant protein A directly interacts with TLR4 and MD-2 and regulates inflammatory cellular response. Importance of supratrimeric oligomerization. *J. Biol. Chem.* 281: 21771–21780.
22. Stamme, C., E. Walsh, and J. R. Wright. 2000. Surfactant protein A differentially regulates IFN- $\gamma$ - and LPS-induced nitrite production by rat alveolar macrophages. *Am. J. Respir. Cell Mol. Biol.* 23: 772–779.
23. Hussain, S., J. R. Wright, and W. J. Martin, II. 2003. Surfactant protein A decreases nitric oxide production by macrophages in a tumor necrosis factor- $\alpha$ -dependent mechanism. *Am. J. Respir. Cell Mol. Biol.* 28: 520–527.
24. Pasula, R., J. R. Wright, D. L. Kachel, and W. J. Martin, II. 1999. Surfactant protein A suppresses reactive nitrogen intermediates by alveolar macrophages in response to *Mycobacterium tuberculosis*. *J. Clin. Invest.* 103: 483–490.
25. Sánchez-Barbero, F., G. Rivas, W. Steinhilber, and C. Casals. 2007. Structural and functional differences among human surfactant proteins SP-A1, SP-A2 and co-expressed SP-A1/SP-A2: role of supratrimeric oligomerization. *Biochem. J.* 406: 479–489.
26. Sánchez-Barbero, F., J. Strassner, R. García-Cañero, W. Steinhilber, and C. Casals. 2005. Role of the degree of oligomerization in the structure and function of human surfactant protein A. *J. Biol. Chem.* 280: 7659–7670.
27. Sáenz, A., A. López-Sánchez, J. Mojica-Lázaro, L. Martínez-Caro, N. Nin, L. A. Bagatoli, and C. Casals. 2010. Fluidizing effects of C-reactive protein on lung surfactant membranes: protective role of surfactant protein A. *FASEB J.* 24: 3662–3673.
28. National Research Council. 1996. *Guide for the Care and Use of Laboratory Animals*. National Academy Press, Washington, D.C. DOI: 10.17226/5140.
29. Casals, C., J. Arias-Diaz, F. Valino, A. Saenz, C. Garcia, J. L. Balibrea, and E. Vara. 2003. Surfactant strengthens the inhibitory effect of C-reactive protein on human lung macrophage cytokine release. *Am. J. Physiol. Lung Cell. Mol. Physiol.* 284: L466–L472.
30. Gea-Sorlí, S., R. Guíllamat, A. Serrano-Mollar, and D. Closa. 2011. Activation of lung macrophage subpopulations in experimental acute pancreatitis. *J. Pathol.* 223: 417–424.
31. de las Casas-Engel, M., A. Domínguez-Soto, E. Sierra-Filardi, R. Bragado, C. Nieto, A. Puig-Kroger, R. Samaniego, M. Loza, M. T. Corcuera, F. Gómez-Aguado, et al. 2013. Serotonin skews human macrophage polarization through HTR2B and HTR7. *J. Immunol.* 190: 2301–2310.
32. Green, M. R., and J. Sambrook. 2012. *Molecular Cloning: A Laboratory Manual*, 4th Ed. Cold Spring Harbor Laboratory Press, Cold Spring Harbor, NY.
33. Livak, K. J., and T. D. Schmittgen. 2001. Analysis of relative gene expression data using real-time quantitative PCR and the 2(- $\Delta\Delta C(T)$ ) method. *Methods* 25: 402–408.
34. Anderson, P., Y. K. Yip, and J. Vilcek. 1982. Specific binding of 125I-human interferon-gamma to high affinity receptors on human fibroblasts. *J. Biol. Chem.* 257: 11301–11304.
35. Sheehan, K. C., J. Calderon, and R. D. Schreiber. 1988. Generation and characterization of monoclonal antibodies specific for the human IFN- $\gamma$  receptor. *J. Immunol.* 140: 4231–4237.
36. Vila-del Sol, V., C. Punzón, and M. Fresno. 2008. IFN- $\gamma$ -induced TNF- $\alpha$  expression is regulated by interferon regulatory factors 1 and 8 in mouse macrophages. *J. Immunol.* 181: 4461–4470.
37. Fang, F. C. 2004. Antimicrobial reactive oxygen and nitrogen species: concepts and controversies. *Nat. Rev. Microbiol.* 2: 820–832.
38. Gross, T. J., K. Kremens, L. S. Powers, B. Brink, T. Knutson, F. E. Domann, R. A. Philibert, M. M. Milhem, and M. M. Monick. 2014. Epigenetic silencing of the human NOS2 gene: rethinking the role of nitric oxide in human macrophage inflammatory responses. *J. Immunol.* 192: 2326–2338.
39. Hussell, T., and T. J. Bell. 2014. Alveolar macrophages: plasticity in a tissue-specific context. *Nat. Rev. Immunol.* 14: 81–93.
40. Sierra-Filardi, E., C. Nieto, A. Domínguez-Soto, R. Barroso, P. Sánchez-Mateos, A. Puig-Kroger, M. López-Bravo, J. Joven, C. Ardavin, J. L. Rodríguez-Fernández, et al. 2014. CCL2 shapes macrophage polarization by GM-CSF and M-CSF: identification of CCL2/CCR2-dependent gene expression profile. *J. Immunol.* 192: 3858–3867.
41. DiSepio, D., C. Ghosn, R. L. Eckert, A. Deucher, N. Robinson, M. Duvic, R. A. Chandraratna, and S. Nagpal. 1998. Identification and characterization of a retinoid-induced class II tumor suppressor/growth regulatory gene. *Proc. Natl. Acad. Sci. USA* 95: 14811–14815.
42. Carella, C., M. Potter, J. Bonten, J. E. Rehg, G. Neale, and G. C. Grosveld. 2006. The ETS factor TEL2 is a hematopoietic oncoprotein. *Blood* 107: 1124–1132.
43. Ealick, S. E., W. J. Cook, S. Vijay-Kumar, M. Carson, T. L. Nagabhushan, P. P. Trotta, and C. E. Bugg. 1991. Three-dimensional structure of recombinant human interferon- $\gamma$ . *Science* 252: 698–702.
44. Ruano, M. L., I. García-Verdugo, E. Miguel, J. Pérez-Gil, and C. Casals. 2000. Self-aggregation of surfactant protein A. *Biochemistry* 39: 6529–6537.
45. Wright, J. R. 1997. Immunomodulatory functions of surfactant. *Physiol. Rev.* 77: 931–962.
46. Ballard, P. L., H. G. Liley, L. W. Gonzales, M. W. Odum, A. J. Ammann, B. Benson, R. T. White, and M. C. Williams. 1990. Interferon- $\gamma$  and synthesis of surfactant components by cultured human fetal lung. *Am. J. Respir. Cell Mol. Biol.* 2: 137–143.
47. Zhang, S. Y., S. Boisson-Dupuis, A. Chapgier, K. Yang, J. Bustamante, A. Puel, C. Picard, L. Abel, E. Jouanguy, and J. L. Casanova. 2008. Inborn errors of interferon (IFN)-mediated immunity in humans: insights into the respective roles of IFN- $\alpha/\beta$ , IFN- $\gamma$ , and IFN- $\lambda$  in host defense. *Immunol. Rev.* 226: 29–40.
48. Ichikawa, A., K. Kuba, M. Morita, S. Chida, H. Tezuka, H. Hara, T. Sasaki, T. Ohteki, V. M. Ranieri, C. C. dos Santos, et al. 2013. CXCL10-CXCR3 enhances the development of neutrophil-mediated fulminant lung injury of viral and nonviral origin. *Am. J. Respir. Crit. Care Med.* 187: 65–77.
49. Jiang, D., J. Liang, R. Guo, T. Xie, F. L. Kelly, T. Martinu, T. Yang, A. K. Lovgren, J. Chia, N. Liu, et al. 2012. Long-term exposure of chemokine CXCL10 causes bronchiolitis-like inflammation. *Am. J. Respir. Cell Mol. Biol.* 46: 592–598.
50. Wang, Z., T. Zheng, Z. Zhu, R. J. Homer, R. J. Riese, H. A. Chapman, Jr., S. D. Shapiro, and J. A. Elias. 2000. Interferon  $\gamma$  induction of pulmonary emphysema in the adult murine lung. *J. Exp. Med.* 192: 1587–1600.
51. Wang, W., P. Yang, Y. Zhong, Z. Zhao, L. Xing, Y. Zhao, Z. Zou, Y. Zhang, C. Li, T. Li, et al. 2013. Monoclonal antibody against CXCL10/IP-10 ameliorates influenza A (H1N1) virus induced acute lung injury. *Cell Res.* 23: 577–580.
52. Wlodarczyk, M. F., A. R. Kraft, H. D. Chen, L. L. Kenney, and L. K. Selin. 2013. Anti-IFN- $\gamma$  and peptide-tolerization therapies inhibit acute lung injury induced by cross-reactive influenza A-specific memory T cells. *J. Immunol.* 190: 2736–2746.
53. Casals, C., A. Varela, M. L. Ruano, F. Valiño, J. Pérez-Gil, N. Torre, E. Jorge, F. Tendillo, and J. L. Castillo-Olivares. 1998. Increase of C-reactive protein and decrease of surfactant protein A in surfactant after lung transplantation. *Am. J. Respir. Crit. Care Med.* 157: 43–49.
54. Martin, T. R. 2000. Recognition of bacterial endotoxin in the lungs. *Am. J. Respir. Cell Mol. Biol.* 23: 128–132.
55. Goto, H., J. G. Ledford, S. Mukherjee, P. W. Noble, K. L. Williams, and J. R. Wright. 2010. The role of surfactant protein A in bleomycin-induced acute lung injury. *Am. J. Respir. Crit. Care Med.* 181: 1336–1344.

# Surfactant protein A prevents IFN- $\gamma$ /IFN- $\gamma$ R interaction and attenuates classical activation of human alveolar macrophages

Reference: 15-01032-FL

Carlos M. Minutti\*†#, Belén García-Fojeda\*†#, Alejandra Sáenz\*†, Mateo de las Casas-Engel‡, Raquel Guillamat-Prats†¶, Alba de Lorenzo\*, Anna Serrano-Mollar†¶, Ángel L. Corbí‡, and Cristina Casals\*†§

---

## Supplemental Data

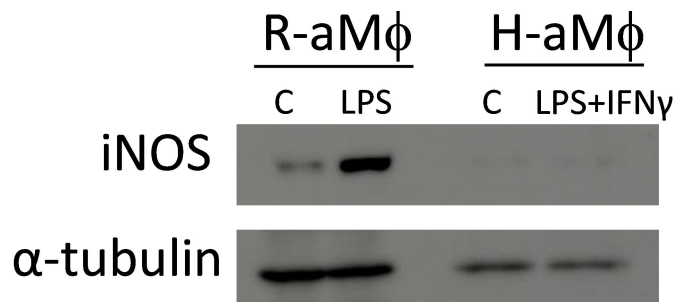


**Figure S1. iNOS protein is not induced upon LPS+IFN- $\gamma$  stimulation in human alveolar macrophages.** Human and rat aM $\phi$  were cultured in the presence or absence of IFN- $\gamma$  (10 ng/ml) and/or LPS (10 ng/ml) for 24 hours. iNOS protein expression was examined by Western blot. A representative Western blot image is shown.

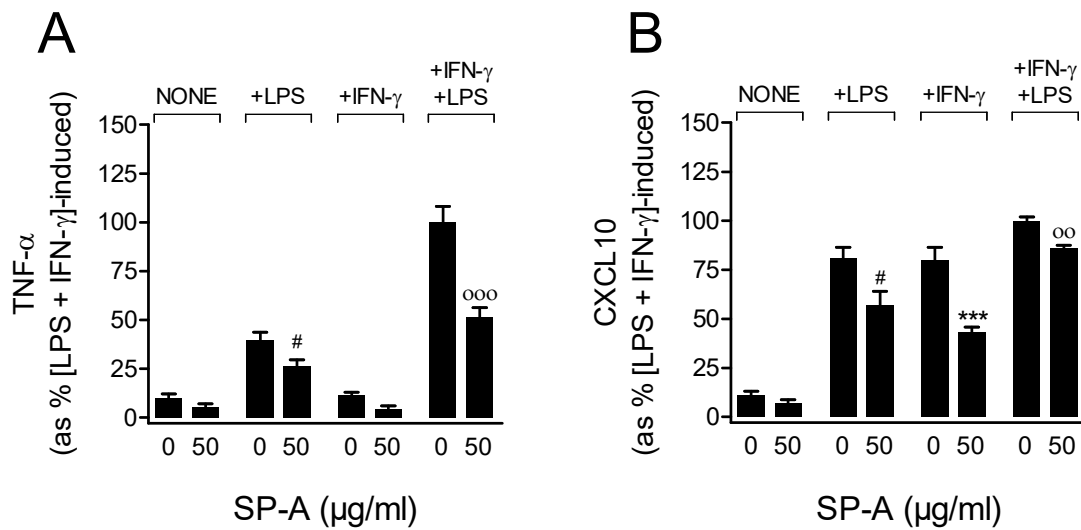


**Figure S2. SP-A inhibits TNF- $\alpha$  and CXCL10 secretion by human M $\phi$ (M-CSF) stimulated with IFN- $\gamma$ , LPS, or IFN- $\gamma$  +LPS.** Human M $\phi$ (M-CSF) were cultured in the presence or absence of IFN- $\gamma$  (0.5 ng/ml), LPS (0.5 ng/ml), SP-A (50  $\mu$ g/ml), and combinations thereof. We measured TNF- $\alpha$  (A) and CXCL10 (B) secretion after 24 h of IFN- $\gamma$  and/or LPS-stimulation. The results are expressed as percent of LPS plus IFN- $\gamma$ -stimulated secretion of TNF- $\alpha$  (A) or CXCL10 (B) in the absence of SP-A. The data shown are means  $\pm$  SEM of four different M $\phi$  cultures. The mean values of LPS + IFN- $\gamma$ -induced TNF- $\alpha$  and CXCL10 secretion in the absence of SP-A were  $2.6 \pm 0.3$  ng/ml and  $21.7 \pm 1.5$  ng/ml, respectively (100 %). <sup>#</sup>P < 0.05, <sup>###</sup>P < 0.001 when compared with the response elicited by LPS without SP-A. \*P < 0.05, \*\*P < 0.01, \*\*\*P < 0.001 when compared with the response elicited by IFN- $\gamma$  in the absence of SP-A. <sup>ooo</sup> P < 0.001 when compared with the response elicited by LPS+IFN- $\gamma$  in the absence of SP-A.